HHS Public Access

Author manuscript

Med Eng Phys. Author manuscript; available in PMC 2017 April 01.

Published in final edited form as:

Med Eng Phys. 2016 April ; 38(4): 411–416. doi:10.1016/j.medengphy.2016.01.011.

Design, Fabrication and Characterization of a Pure Uniaxial Microloading System for Biologic Testing

Jonathan D. King[a], **Spencer L. York**[a], and **Marnie M. Saunders**[a]

Jonathan D. King: jdk31@zips.uakron.edu; Spencer L. York: sly15@zips.uakron.edu; Marnie M. Saunders: mms129@uakron.edu

[a]Department of Biomedical Engineering, The University of Akron, 302 E Buchtel Ave, Akron, OH 44325-0302, United States

Abstract

The field of mechanobiology is aimed at understanding the role the mechanical environment plays in directing cell and tissue development, function and disease. The empirical aspect of the field requires the development of accurate, reproducible and reliable loading platforms that can apply microprecision mechanical load. In this study we designed, fabricated and characterized a pure uniaxial loading platform capable of testing small synthetic and organic specimens along a horizontal axis. The major motivation for platform development was in stimulating bone cells seeded on elastomeric substrates and soft tissue loading. The biological uses required the development of culturing fixtures and environmental chamber. The device utilizes commercial microactuators, load cells and a rail/carriage block system. Following fabrication, acceptable performance was verified by suture tensile testing.

Keywords

mechanobiology; biologic sample loading; mechanical loading device design; biomedical testing; device characterization

Introduction

The body is continually in a state of loading. As such, cells at the microscopic scale reside in highly dynamic environments and are subjected to a variety of loading modes [1]. The loads are believed to be critical to cell development, function and survival. For example, cell differentiation, migration and signal transduction are influenced by mechanical loading [2–3]. Mechanical forces are particularly critical to bone cells, and it is known that mechanical forces at least in part, regulate bone remodeling [4–6]. Given that the mechanisms and pathways by which bone cells coordinate activity in response to normal loading have yet to

Conflicts of Interest - None

Ethical Approval – Not required

be elucidated, research aimed at understanding the role of load in bone disease (eg, osteoporosis), overload and disuse must first focus on understanding the role physiologic loading plays in bone adaptation. *In vivo* these mechanisms can be difficult to test and observe. *In vitro* systems offer the opportunity to investigate these mechanisms and pathways of interest in an isolated, simplified environment [7–8].

To mechanically load cells in a biomimetically appropriate environment, specialized platforms are often fabricated in-house [3, 5, 9–16]. Commercial platforms can be cost prohibitive and customization is highly dependent upon user expertise [13–15]. Most commercial loading machines work off the principle of a fixed platform and one mover on a central axis. During testing, specimens are clamped in fixtures such that one end of the specimen is fixed to the stationary base of the platform and one end is attached to the mover. As such, tension/compression testing in a commercial machine is not pure, or equal and opposite. Since the exact mechanical loading patterns experienced by cells are difficult to replicate, creating the most uniform loading possible, such as in pure loading, is important. This will begin to allow us to correlate cellular activity to specific loading patterns. Ultimately, the goal would be to adequately simulate and verify complex *in vivo* loading scenarios. The goal of this study was to design, fabricate and characterize performance of a microactuated pure uniaxial loading platform for straining bone cells seeded on polydimethylsiloxane (PDMS). However, given that the platform was intended as a generic system, it could be used to test a variety of small specimens in pure tension/compression. As such, once fabricated device performance was initially characterized/validated with suture testing.

Methods

A pure uniaxial platform was designed. The device centered around 2 commercial microactuators, 2 commercial load cells and 1 rail/carriage block system. The microactuators (Zaber Technologies) were selected to provide the necessary resolution and smooth motion. To accommodate a variety of potential uses, 2 sets of microactuators were purchased with either a 30mm (NA11B30) or 60mm (NA11B60) travel range. Both models had a 67 N force capacity, 58 N peak thrust, 0.9302 μm/s speed resolution and either a 25 μm (NA11B30) or a 36 μm (NA11B60) unidirectional accuracy. The microactuators utilized a precision lead screw drive mechanism, stepper motor and a 24 V controller (A-MCA, Zaber Technologies). Canister load cells (44.5 N, Honeywell, Sensotec) were selected for their small profile, robustness and user familiarity. The rail/carriage block system (9184T31, McMaster Carr) was selected as a convenient and cost effective way to ensure pure uniaxial loading on center. The maintenance-free system uses two ball bearing carriages that ride on a 15 mm wide track, has a 7800 N dynamic load capacity and is corrosion resistant (400 series stainless steel). The commercial components were purchased and the platform was designed to accommodate them.

The goal of the platform was to apply equal, uniaxial strains (linear displacement) to small-scale specimens in an accurate and reproducible manner. This included ensuring that pre-load was not applied during manipulation of the samples pre-testing. In addition the platform was designed to accommodate synthetic (fibers) and biological (tissues) materials.

For the latter, an environmental chamber and fluid reservoir were fabricated. A horizontal loading approach was selected for easy submersion of the samples during testing given that a major focus of the device was cell stimulation research.

Device Main Wall

The dimensions of the commercial components dictated the design and scale of the platform. All fabricated components were machined from stock aluminum 6061-T6. The basic design consisted of a base plate and 2 side (left and right) plates, Figure 1a–b. A track was machined into the base plate to accommodate the thickness of the side plates and maintain alignment, Figure 2a–c. Clearance holes were drilled through the bottom of the base plate in the track to secure each side plate via holes that were drilled and tapped. A track was machined into the front face of each of the side plates to mount the rail of the commercial rail/carriage system. In addition, a series of drilled and tapped holes on the front face flanked the track to accommodate the actuator mount, Figure 2b. These holes allowed for placement adjustability of the actuator mount and spanned the entire length of each side plate. This allowed objects ranging in gauge length from 1 mm to several cms to be tested on the same platform. The commercial rail was attached to the track using the mounting (clearance) holes in the rail and drilling and tapping holes in the side plate track. The rail was mounted stationary between the side plates. The 2 side plate approach in comparison to 1 large side plate was selected to provide clearance in the event that an overhead camera was required in future testing. The rail/carriage system was purchased as a unit and consisted of 1 rail and 2 carriages. Each carriage mounted one actuator to the rail.

Friction Clamps and Brace

Although the platform can be used for pure compression testing, it was designed for tensile loading of soft tissues, synthetic fibers and cell-seeded elastomers. To this end, serrated friction grips were fabricated for tensile testing specimens; compression platens were not fabricated. The serrated grips, Figure 1c–e, consisted of a left and right fixture with each fixture made up of a top and bottom piece. The fixtures were machined from Plexiglas and the serrations were milled on the face using a double angle cutter (90°). Given that a major purpose of the platform is to subject small tissues and bone cells seeded on PDMS to precise strain, there was concern that the manipulation loads applied to the specimens in setting up the test could exceed those applied during the test. To avoid unintended preloads, a polycarbonate brace was developed to mount between the right and left fixtures. For cell work, the PDMS substrates were clamped in the fixtures and the cells were then seeded on the substrate. Stainless steel screws were used and 5 sets of the fixtures and braces were fabricated to accommodate preparation of multiple samples at the same time. Fixtures were able to be sterilized with alcohol and UV light before each use.

Actuator Mounts

Each actuator used two mounts, a rear mount and a front mount. The stationary rear mount, previously described, connected the actuator body to the side plate via the track, Figure 2. The front mount attached the tip of the actuator to the carriage block via connectors that accommodated the load cells, Figure 3a–c. The front and rear mounts were machined from 6061-T6 aluminum 90° angle stock. To ensure reproducible alignment of the angle stock in

the track (rear mount), a key was made on the underside of the mount by adding a rectangular plate to the base, Figure 2e. The plate rode in a track machined to maintain alignment. This was done to maintain alignment, ensure in-line linear movement of the actuators and minimize user variability in setup. The slotted rear mount enables the microactuator to be attached anywhere along the side plate.

In addition to the front actuator mount providing actuator support and alignment, it also holds a mounted plate with a vertical track, Figure 3d–e. The vertical track provides alignment and holds the slotted plate to which the specimen fixtures attach. The vertical slot in the plate enables adjustable clamp height, Figure 3d. This was done to enable testing of dry and wet specimens. At the lowest point on the track, the specimen can be completely submerged in a bath (cell medium, saline) and environmental chamber controlling for temperature, pH and humidity. Once setup is complete, the plate is locked in position for the duration of the test. Feeler gauges and gauge blocks are used in combination to set height on the right and left fixtures.

Load Cell Attachments

To accommodate the thread sizes of the commercial load cells and enable attachment to the actuators, round aluminum stock was drilled and tapped on end to accept either the threaded actuator tip or the load cell connector, Figure 3c. To anchor the tip of the microactuator to the carriage block one of the round connectors was turned down to provide the clearance and alignment to the front actuator mount. A crude nut with flats was machined to anchor the assembly given the confined space, Figure 3b–c.

Actuators

Once assembled, the platform was run by controlling microactuator motion. The microactuators were controlled using the computer software Zaber Counsel. The proprietary software utilized code written in C Sharp, Visual Basic or Java. Codes were written in order to move specified distances based on desired strain.

Microactuator performance was characterized for travel distance, speed and cyclic temperature. To verify travel accuracy, an arbitrary distance was input and physical measurements of actuator tip displacement were made using feeler gauges with distances ranging between 254–2540 μm. These distances were chosen to represent the desired 1–10% strain range used in our cell work. Speed tests were performed using arbitrary speeds and timing actuator motion. Input speeds ranged from 1–28000 μm/s with actuator travel ranging from 10–56000 μm. Speeds and distances were selected to span the range of actuator performance. For each speed test actuators were extended and retracted in one full cycle. The actuator travel time was measured and compared to the calculated travel time from the inputted speed and distance. To verify overheating was not a concern, each actuator was cycled for 1 hr at maximum speed and distance with temperature recorded at 5 minute intervals. All tests were repeated a minimum of 3 times.

Device Characterization Testing

To verify accurate and reliable performance of the device, suture break testing was conducted using the new platform and the results compared to identical tests conducted in a uniaxial loading machine developed in-house and previously validated [16]. Suture was utilized to establish proof-of-concept for this device due to its simple and consistent geometry. For this test, 10 Ethicon 2-0 silk suture samples were loaded to failure in each loading device. Samples were knotted with 3 knots tied on top of each other to create a stress riser and concentrate failure to the knot and away from the fixtures. To minimize any fixture variability, the fixtures fabricated (Figure 1c–e) were used in both loading devices. A gauge length of 25.4 mm was used (knot placed centrally) with a loading rate of 1.22 mm/sec. Given that the in-house machine previously developed utilized one mover and a fixed based, the pure uniaxial platform was first tested locking in one actuator to simulate the fixed base. The load was measured using a 44.5 N load cell. The failure performance of the two sets of sutures was compared statistically for stiffness, failure load and displacement at failure using two-tailed Mann-Whitney t-tests.

For pure uniaxial testing, 10 sutures were loaded to failure. Both actuators were used at ½ speed of 0.61 mm/s to generate a pure load on the sample at the same rate used in the previous tests. Data was collected using two 44.5 N load cells. Samples were knotted in the same manner and the same 3 parameters were measured.

Results

Microactuator distance and speed performance tests were analyzed using linear regression. In both cases, an r^2 value > 0.999 was obtained when an intercept of 0 was set. The results were also compared to the input values to find deviation, Table 1. Results for the distance tests remained under 4% deviation from the input, and results for speed tests remained under 10% deviation from the inputs. The temperature tests determined that the actuator temperatures never exceeded 40°C over the course of the 1 hr tests with an observed maximum temperature of 39.9°C.

For suture break comparisons, a representative load-displacement curve from samples broken using each loading platform is provided, Figure 4a. Each sample tested failed at the knot located in the center of the gauge length. Stiffness, maximum load and displacement at failure were used to compare results between devices. These measurements showed no statistically significant differences at a 95% confidence interval between the samples as a function of loading machine, Figure 4b–d. Once it was determined that the pure uniaxial platform when operating as a fixed end platform performed similarly to a fixed end loading platform, the pure uniaxial performance was evaluated. As shown in Figure 4e, identical load-displacement curves were generated for the two actuators during application of a pure load. In addition, failure loads, stiffness and displacements were similar to those found in the previous tests. Statistics were not conducted between the fixed axis end and pure uniaxial tests as the comparisons are not appropriate.

Discussion

The goal of this study was to design, fabricate and characterize a pure uniaxial loading device for small-scale specimens, such as fibers, tissues and cell-seeded elastomers. This device was designed to be simple, reliable and cost-effective with the flexibility to grow with a user's testing needs. Loading platforms such as these are an important part of biomedical research laboratories. Here we demonstrate the development of a platform motivated by a biological need. From the tests outlined in this study, we were able to design, construct and validate an accurate, reproducible and therefore reliable small-scale pure uniaxial loading device. The device enables equal and opposite loading of synthetic and biologic specimens on a horizontal axis in wet and dry environments. The microactuator characterization verified the necessary precision required for our intended work and that system performance adequately applies pure uniaxial load to small-scale specimens.

From comparison of the suture results from the fixed axis tests it was determined that the devices were comparable in performance given that there was not a statistically significant difference in structural properties. From the results of the pure uniaxial loading it was determined that load cell performance was identical. This further suggests that pure uniaxial testing was accomplished, including adequate alignment and synchronization of the microactuator travel.

The testing of small-scale specimens in the biomedical engineering field is becoming routine. However commercial systems can be cost-prohibitive when investment is weighed against intended use. For example, the FX-4000 Flexcell and STB-150 Strex systems cost more than $10,000 [14] while the Bose ElectroForce BioDynamic Test Instrument can exceed $50,000 [15]. As such, more and more researchers are developing their own systems to meet their mechanical testing needs within budgetary constraints. Inasmuch as the machining was done in-house using aluminum stock, the only expenses incurred were the cost of the commercial components which were under $4000.00. Given that these commercial components meet the most critical needs of the fixture, reliable movement, load and guaranteed alignment, it is not overly challenging to design and fabricate these platforms. Platform design essentially reduces to physically connecting the commercial components. Furthermore, in stimulating scaffolds and sheets, such as required in soft tissue research, planar biaxial loading is utilized. A pure uniaxial system could be augmented with a second system to create a cost-effective biaxial machine. Utilizing similar approaches, a wide variety of specialized platforms and machines can be fabricated to meet user-specific testing needs.

Acknowledgments

Funding for this project was provided by National Institutes of Health (AREA) and National Science Foundation (Career) awards. The authors would like to thank Mr Larry Saunders and Mr Dale Ertley for machining services, as well as Dustin Hayes for assistance with mechanical testing. Researchers interested in fabrication of their own device are welcome to contact the authors for device technical drawings.

References

1. Ingber DE. Tensegrity: the architectural basis of cellular mechanotransduction. Annu Rev Physiol. 1999; 59(1):575–599. [PubMed: 9074778]
2. Katsumi A, Orr AW, Tzima E, Schwartz MA. Integrins in mechanotransduction. J Biol Chem. 2004; 279(13):12001–12004. [PubMed: 14960578]
3. Riehl BD, Park JH, Kwon K, Lim JY. Mechanical stretching for tissue engineering: Two-dimensional and three-dimensional constructs. Tissue Eng. 2012; 18(4):288–300.
4. Burr, DB.; Allen, MR. Basic and applied bone biology. San Diego: Academic Press; 2014. p. 80-84.
5. Li J, Wan Z, Liu H, Li H, Liu L, Li R, Guo Y, Chen W, Zhang X, Zhang X. Osteoblast subjected to mechanical strain inhibit osteoclastic differentiation and bone resorption in a co-culture system. Ann Biomed Eng. 2013; 41(10):2056–2066. [PubMed: 23609024]
6. Oers RFM, Wang H, Bacabac RG. Osteocyte shape and mechanical loading. Curr Osteoporos Rep. 2015; 13:61–66. [PubMed: 25663071]
7. Brown TD. Techniques for mechanical stimulation of cells in vitro: a review. J Biomech. 2000; 33(1):3–14. [PubMed: 10609513]
8. Davis CA, Zambrano S, Anumolu P, Allen ACB, Sonoqui L, Moreno MR. Device-based in vitro techniques for mechanical stimulation of vascular cells: a review. J Biomech Eng. 2015; 137(4): 040801. [PubMed: 25378106]
9. Keyes JT, Haskett DG, Utzinger U, Azhar M, Vander Geest JP. Adaptation of a planar microbiaxial optomechanical device for the tubular biaxial microstructural and macroscopic characterization of small vascular tissues. J Biomech Eng-T ASME. 2011; 133(7):075001.
10. Huang Y, Nguyen NT, Lok KS, Lee PPF, Su M, Wu M, Kocqozlu L, Ladoux B. Multiarray cell stretching platform for high-magnification real-time imaging. Nanomedicine. 2013; 8(4):543–553. [PubMed: 23560406]
11. Kim HJ, Huh D, Hamilton G, Ingber DE. Human gut-on-a-chip inhabited by microbial flora that experiences intestinal peristalsis-like motions and flow. Lab on a Chip. 2012; 12:2165–2174. [PubMed: 22434367]
12. Delaine-Smith RM, Javaheri B, Edwards JH, Vazquez M, Rumney RMH. Preclinical models for *in vitro* mechanical loading of bone-derived cells. BoneKEy Reports. 2015; 4:728. [PubMed: 26331007]
13. Wang T, Gardiner BS, Lin Z, Rubenson J, Kirk TB, Wang A, Xu J, Smith DW, Lloyd DG, Zheng MH. Bioreactor design for tendon/ligament engineering. Tissue Eng. 2013; 19(2):133–146.
14. Iwadate Y, Yumura S. Cyclic stretch of the substratum using a shape-memory alloy induces directional migration in dictyostelium cells. Biotechniques. 2009; 47(3):757–767. [PubMed: 19852761]
15. Huang AH, Lee YU, Calle EA, Boyle M, Starcher BC, Humphrey JD, Niklason LE. Design and use of a novel bioreactor for regeneration of biaxially stretched tissue-engineered vessels. Tissue Eng. 2015; 21(8):841–851.
16. Saunders M, Donahue H. Development of a cost-effective loading machine for biomechanical evaluation of mouse transgenic models. Med Eng Phys. 2004; 26:596–603.

Highlights

- A device for pure uniaxial microloading of biologic samples was designed.
- Design restrictions included low cost, biologic compatibility and reliability.
- This device was verified by comparison to an existing device.
- This low costs device replaces the need of standard cost prohibitive devices.

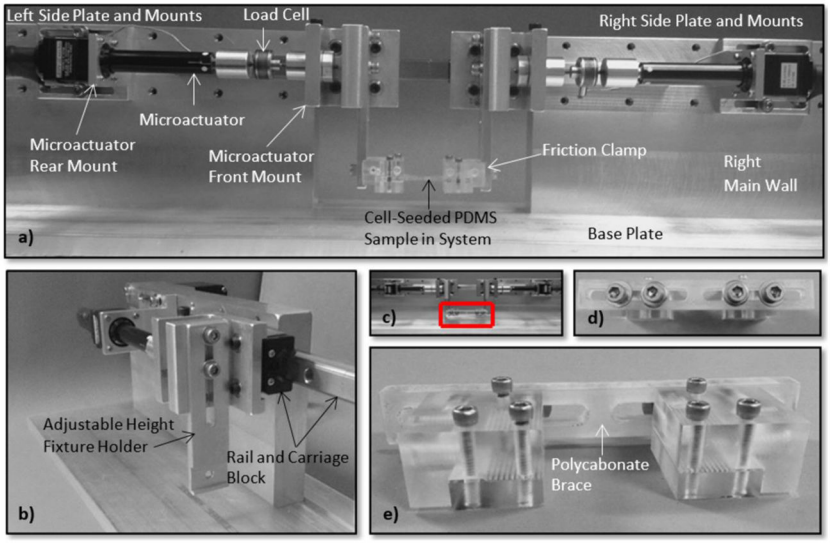

Figure 1.

a,b) A pure uniaxial loading platform was designed around commercial components and fabricated from aluminum 6061-T6. c–e) Friction clamps with polycarbonate brace to eliminate unintended loading effects during manipulation of the sample before experimentation.

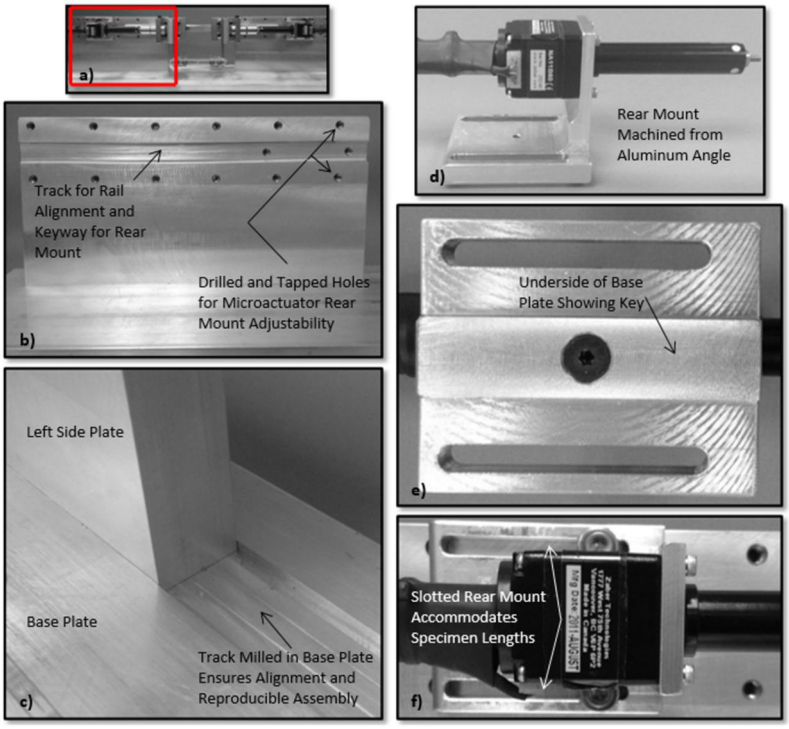

Figure 2.

a) Main wall of the device includes b) a slot for alignment of the guide rail and actuator mounts. c) Left (shown) and right side plates connect to the base plate using holes on the underside of the base plate and a track for alignment. d–f) Rear actuator mount for attaching actuators to the side plate machined from aluminum angle stock. e) A key was used to align the mounts to the side plate. f) Slots allow for simple adjustment of the actuator position while remaining in-line with the guide rail.

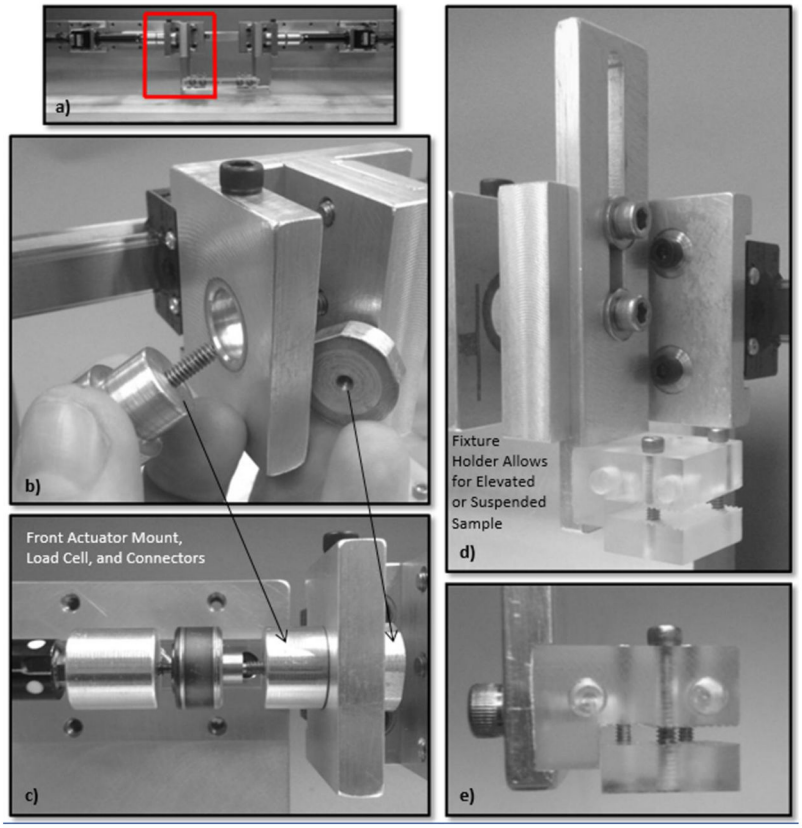

Figure 3.

a–c) Connectors for attaching load cells to the actuator and front actuator mount. b) Nuts were fabricated due to the small working space. d) Adjustable slotted plate fixture for elevating or suspending samples into a heated media bath during testing. e) The holder had a track machined to provide a recess to hold the Plexiglas friction clamps.

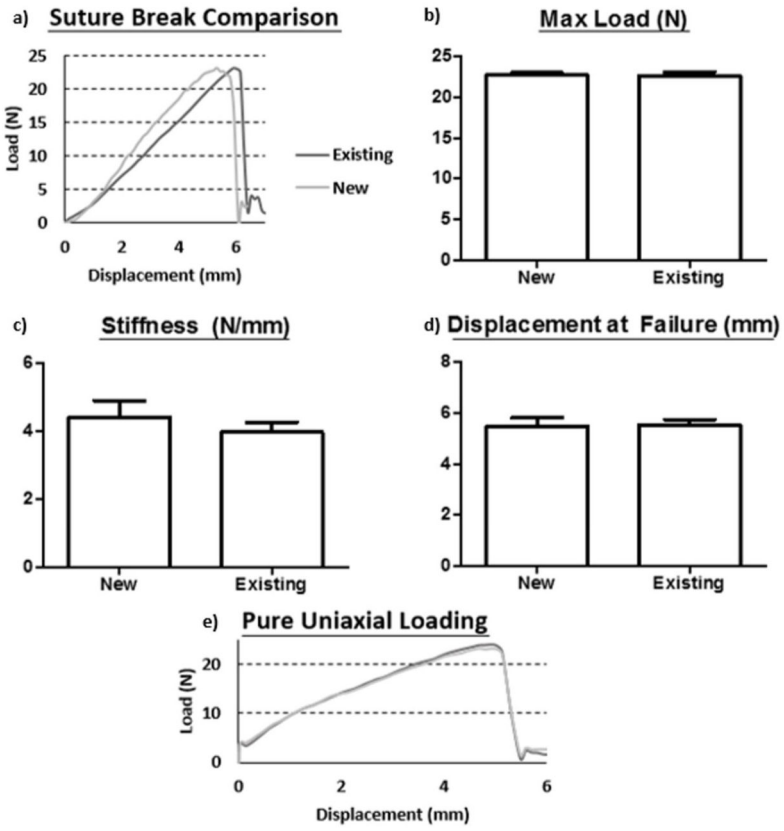

Figure 4.

a) Representative data from the suture break test showed b–d) no significant difference in the max load, stiffness or displacement at failure. e) Pure uniaxial load-displacement curve generated from suture testing to failure.

Table 1

Average distance and speed accuracy test results. Standard deviations calculated from result's deviation from input.

Distance Accuracy						
	Input Distance (μm)	**Measured Distance (μm)**	**Deviation from Input (%)**	**Standard Deviation**		
30mm Actuators	254	263.2	3.6	0.02		
	635	641.4	1.0	0.01		
	1270	1260.7	0.7	0.01		
	2540	2536.9	0.1	0.01		
Speed Accuracy						
	Input Distance (μm)	**Input Speed (μm/s)**	**Calculated Time (s)**	**Measured Time (s)**	**Deviation of Results (%)**	**Standard Deviation**
30mm Actuators	1,000	10	200	218	9.0	0.0
	20,000	10,000	40	42.8	6.9	0.1
	30,000	15,000	4	4.4	9.5	0.0
60mm Actuators	10	1	20	21.9	9.3	0.2
	1,000	10	200	218.5	9.3	0.7
	56,000	14,000	8	8.3	3.8	1.8